Inorganic Chemistry

Article

pubs.acs.org/IC

Synthesis, Crystal Structure, and Luminescent Properties of 2-(2,2,2-Trifluoroethyl)-1-indone Lanthanide Complexes

Jingya Li, Hongfeng Li, Pengfei Yan,* Peng Chen, Guangfeng Hou, and Guangming Li*

Key Laboratory of Functional Inorganic Material Chemistry (MOE), School of Chemistry and Materials Science, Heilongjiang University, No. 74, Xuefu Road, Nangang District, Harbin 150080, People's Republic of China

Supporting Information

ABSTRACT: A new β-diketone, 2-(2,2,2-trifluoroethyl)-1-indone (TFI), which contains a trifluorinated alkyl group and a rigid indone group, has been designed and employed for the synthesis of two series of new TFI lanthanide complexes with a general formula $[Ln(TFI)_3L]$ [Ln = Eu, L = $(H_2O)_2$ (**1**), bpy (**2**), and phen (**3**); Ln = Sm, L = $(H_2O)_2$ (**4**), bpy (**5**), and phen (**6**); bpy = 2,2′-bipyridine, phen = 1,10-phenanthroline]. X-ray crystallographic analysis reveals that complexes **1**−**6** are mononuclear, with the central Ln^{3+} ion eight-coordinated by six oxygen atoms furnished by three TFI ligands and two O/N atoms from ancillary ligand(s). The room-temperature photoluminescence (PL) spectra of complexes **1**−**6** show strong characteristic emissions of the corresponding Eu^{3+} and Sm^{3+} ions, and the substitution of the solvent molecules by bidentate nitrogen ligands essentially enhances the luminescence quantum yields and lifetimes of the complexes.

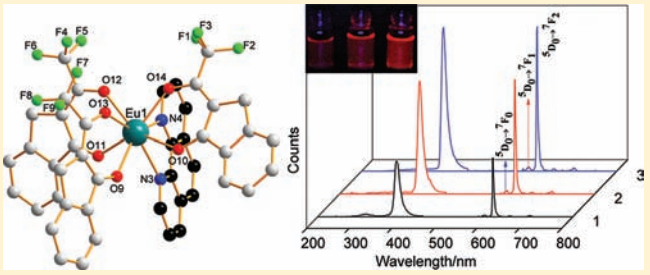

INTRODUCTION

The various photophysical properties of lanthanide ions have inspired vigorous research activities because of the wide range of photonic applications, such as tunable lasers, amplifiers for optical communications, luminescent probes for analyses, components of the emitting materials in multilayer organic light emitting diodes, and efficient light conversion molecular devices.[1−6] The Eu^{3+} and Tb^{3+} ions are of particular interest because of their long luminescence lifetime and narrow emission bands in the visible region.[7] The wide use of Eu^{3+} ions is also due to a variety of spectroscopy reasons, for instance, simple electronic structure, local probe, presence of a magnetic dipole transition, etc.[8] Because the Laporte−forbidden 4f−4f transition prevent direct excitation of the luminescence of the lanthanide, Ln^{3+} ions always require sensitization by suitable organic chromophores. Therefore, Ln^{3+} ions must be incorporated into highly stable coordinated complexes for practical applications. The efficiency of ligand-to-metal energy transfer, which requires compatibility between the energy levels of the ligand excited states and accepting levels of the Ln^{3+} ions, is crucial in the design of high performance luminescent molecular devices. β-diketones are among the most important ligands for lanthanide luminescence purposes, because they are able to form stable adducts with Ln^{3+} ions and are of strong absorption within a large wavelength range for its $\pi-\pi^*$ transition that may sensitize the luminescence of the Ln^{3+} ions as an "antenna",[9] which can be effectively transferred to the Ln^{3+} ions, resulting in high efficiency emissions.

In addition, ligands containing high-energy oscillators, such as C−H, O−H, and N−H bonds, are able to quench the metal excited states nonradiatively, resulting in lower luminescence intensities and shorter excited-state lifetimes. Thus, the replacement of C−H bonds with C−F bonds is important in the design of new luminescent lanthanide complexes with regard to the efficient emission and the heavy-atom effect, which facilitates intersystem crossing and could enhance the lanthanide-centered luminescence.[10,11] Furthermore, a high value of luminescence quantum yields is generally associated with ligands possessing an extensive delocalized system of conjugated double bonds that results in a relatively rigid structure. The rigid ligand restricts the thermal vibration of the complexes and reduces the loss of energy by nonradiative decay.[12−14]

On the basis of the above-mentioned consideration, we have designed and synthesized a new β-diketone, 2-(2,2,2-trifluoroethyl)-1-indone (TFI), which is composed of the trifluorinated alkyl group and the rigid indone group.[15−19] In view of the positive effect of ancillary nitrogen ligands, such as bpy[20] and phen,[21] on the quantum yields and lifetimes of β-diketone lanthanide complexes, two series of TFI lanthanide complexes containing bpy and phen have been isolated and their photophysical properties are expatiated.

EXPERIMENTAL SECTION

Materials and Instrumentation. Europium oxide (Eu_2O_3, 99.99%), gadolinium oxide (Gd_2O_3, 99.99%), and samarium oxide (Sm_2O_3, 99.99%) were purchased from Ji Nan Rare Earth Chemical Plant (Shandong, China). Sodium hydride (60%, A. R.), 2,2′-bipyridine (98%, A. R.), and 1,10-phenanthroline monohydrate (99%, A. R.) were purchased from Beijing Fine Chemical Co. (Beijing,

Received: November 16, 2011
Published: April 20, 2012

   dx.doi.org/10.1021/ic202473b | Inorg. Chem. 2012, 51, 5050−5057

Scheme 1. Synthesis of the TFI

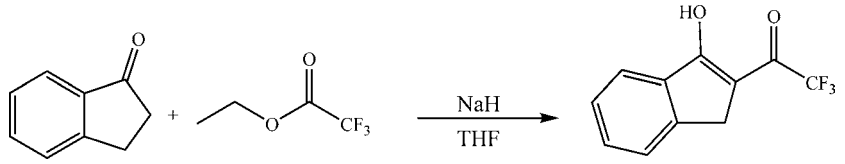

China), 1-indone and ethyl trifluoroacetate were purchased from Shanghai D&R Fine Chem Co. (Shanghai, China). All these reagents were used directly without further purification. $LnCl_3{\cdot}6H_2O$ was prepared according to the literature by dissolving lanthanide oxide in a slight excess of hydrochloric acid. The solution was evaporated and the precipitate was collected from water.[10]

Fourier transform infrared (FT-IR) spectra were obtained on a Perkin-Elmer Spectrum One spectrophotometer by using KBr disks in the range 4000−450 cm^{-1}. Ultraviolet (UV) spectra were recorded on a Perkin-Elmer Lambda 25 spectrometer. Thermal analyses were conducted on a Perkin-Elmer STA 6000 with a heating rate of 10 °C·min^{-1} in a temperature range from 30 to 800 °C under atmosphere. The ^1H NMR spectra were recorded on a Bruker Avance III 400 MHz spectrometer in $CDCl_3$ solution. Excitation and emission spectra were measured with an Edinburgh FLS 920 fluorescence spectrophotometer. Luminescence lifetimes were recorded on a single photon counting spectrometer from Edinburgh Instrument (FLS 920) with microsecond pulse lamp as the excitation. The data were analyzed by software supplied by Edinburgh Instruments. The luminescence quantum yields of the europium complexes were measured in CH_3CN at room temperature and cited relative to a reference solution of $Ru(bpy)_3Cl_2$ (Φ = 55.3%),[22] and they were calculated according to the well-known equation:

$$\varphi_{overall} = \frac{n^2 A_{ref} I}{n_{ref}^2 A I_{ref}} \varphi_{ref} \quad (1)$$

In eq 1, n, A, and I denote the refractive index of solvent, the area of the emission spectrum, and the absorbance at the excitation wavelength, respectively, and φ_{ref} represents the quantum yield of the standard $Ru(bpy)_3Cl_2$ solution. The subscript ref denotes the reference, and the absence of a subscript implies an unknown sample.

Synthesis of 2-(2,2,2-Trifluoroethyl)-1-indone (TFI). A typical procedure of Claisen condensation was used, as shown in Scheme 1. 1-Indone (0.98 g, 7.5 mmol) and ethyl trifluoroacetate (1.08 g, 7.5 mmol) were added into THF (150 mL), and the mixed solution was allowed to stir for 10 min. To this solution, NaH (0.32 g, 7.5 mmol) was added under an inert atmosphere and allowed to stir for 24 h at room temperature. The resulting solution was quenched with water and acidified to pH 2−3 using hydrochloric acid (2 M solution). Then, the suspension was extracted twice with CH_2Cl_2 (70 mL). The organic layer was dried over Na_2SO_4, and the solvent was evaporated leading to a maroon oily solid. The buff solid product was isolated by recrystallization from dichloromethane and hexane (1.36 g, yield of 79% based on 1-idenone). Elemental analysis (%) calcd for $C_{11}H_7F_3O_2$ (228.20): C, 57.90; H, 3.09. Found: C, 57.87; H, 3.07. IR (KBr) ν_{max}: 3430 cm^{-1} (s, ν_{O-H}), 1688 cm^{-1} (s, $\nu_{C=O}$), 1325 cm^{-1} (s), 1270 cm^{-1} (s), 1137 cm^{-1} (s, ν_{C-F}), 751 cm^{-1} (m, ν_{CF_3}). ^1H NMR ($CDCl_3$, 400 MHz): 15.20 (s, 1H), 7.88 (d, J = 4.75 Hz, 1H), 7.67 (t, J = 4.75 Hz, 1H), 7.56 (d, J = 4.75 Hz, 1H), 7.49 (t, J = 4.75 Hz, 1H), 3.83 (s, 1H) (Figure S1, Supporting Information). m/z = 228 (M^+) (Figure S2, Supporting Information).

Synthesis of NaTFI. To a 50 mL methanol solution containing TFI (1.0 mmol), NaOH (2.0 mmol) was added under constant stirring for 1 h at room temperature. The resulting solution was filtered to obtain a white powder. Elemental analysis (%) calcd for $C_{11}H_9F_3Na_2O_2$ (276.20): C, 47.84; H, 3.28. Found: C, 47.82; H, 3.30. IR (KBr) ν_{max}: 1687 cm^{-1}(s, $\nu_{C=O}$), 1323 cm^{-1} (s), 1272 cm^{-1} (s), 1134 cm^{-1} (s, ν_{C-F}), 751 cm^{-1} (m, ν_{CF_3}).

Synthesis of $Gd(TFI)_3(H_2O)_2$. An aqueous solution of $GdCl_3{\cdot}6H_2O$ (0.5 mmol) was added to a solution of TFI (1.5 mmol) in ethanol in the presence of NaOH (1.5 mmol). Precipitation took place immediately, and the reaction mixture was stirred for 10 h at room temperature. The product was filtered, washed with ethanol, washed with water, and then washed with ethanol, dried, and stored in a desiccator. The complex was then purified by recrystallization from a dichloromethane−ethanol mixture. Yield: 82%. Elemental analysis (%) calcd for $C_{33}H_{22}GdF_9O_8$ (874.80): C, 45.31; H, 2.53. Found: C, 45.33; H, 2.51. IR (KBr) ν_{max}: 3424 cm^{-1} (s, ν_{O-H}), 1631 cm^{-1} (s, $\nu_{C=O}$), 1328 cm^{-1} (s), 1279 cm^{-1} (s), 1128 cm^{-1} (s, ν_{C-F}), 754 cm^{-1} (m, ν_{CF_3}).

Synthesis of $Gd(bpy)_2(NO_3)_3$. To a 50 mL ethanol solution containing 2,2′-bipyridine (2.0 mmol), $Gd(NO_3)_3(H_2O)_6$ (1.0 mmol) was added dropwise under constant stirring, and then, the solution was refluxed for 1 h at 80 °C. The resulting solution was filtered to obtain a white powder. Elemental analysis (%) calcd for $C_{20}H_{20}GdN_6O_6$ (597.70): C, 40.19; H, 3.37; N, 14.06. Found: C, 40.17; H, 3.39; N, 14.05. IR (KBr) ν_{max}: 1578 cm^{-1} (s, ν_{N-O}), 1458 cm^{-1} (s), 1415 cm^{-1} (s), 1312 cm^{-1} (s), 1039 cm^{-1} (s, ν_{C-N}), 757 cm^{-1} (m, ν_{N-O}).

Synthesis of $Gd(phen)_2(NO_3)_3$. To a 50 mL ethanol solution containing 1,10-phenanthroline (2.0 mmol), $Gd(NO_3)_3(H_2O)_6$ (1.0 mmol) was added dropwise under constant stirring, and then, the solution was refluxed for 1 h at 80 °C. The resulting solution was filtered to obtain a white powder. Elemental analysis (%) calcd for $C_{24}H_{20}GdN_6O_6$ (645.70): C, 44.64; H, 3.12; N, 14.87. Found: C, 44.67; H, 3.10; N, 14.85. IR (KBr) ν_{max}: 1559 cm^{-1} (s, ν_{N-O}), 1422 cm^{-1} (s), 1295 cm^{-1} (s), 1026 cm^{-1} (s, ν_{C-N}), 739 cm^{-1} (m, ν_{N-O}).

Synthesis of 1 and 4. To a methanol solution of TFI (2.02 g, 8.8 mmol), NaOH (0.35 g, 8.8 mmol) was added, and the mixture was allowed to stir for 5 min. To this methanol solution, $LnCl_3{\cdot}6H_2O$ (2.9 mmol) was added dropwise, and the mixture was allowed to stir for 24 h at ambient temperature. Water was then added to this mixture, and the precipitate thus formed was filtered, washed with water, and dried in air. Single crystals were obtained in about two weeks by recrystallization from CH_2Cl_2/hexane.

$Eu(TFI)_3(H_2O)_2$ (1). Yield: 87%. Elemental analysis (%) calcd for $C_{33}H_{22}EuF_9O_8$ (869.47): C, 45.59; H, 2.55. Found: C, 45.58; H, 2.53. IR (KBr) ν_{max}: 3427 cm^{-1} (s, ν_{O-H}), 1630 cm^{-1} (s, $\nu_{C=O}$), 1328 cm^{-1} (s), 1279 cm^{-1} (s), 1132 cm^{-1} (s, ν_{C-F}), 754 cm^{-1} (m, ν_{CF_3}).

$Sm(TFI)_3(H_2O)_2$ (4). Yield: 84%. Elemental analysis (%) calcd for $C_{33}H_{22}SmF_9O_8$ (867.86): C, 45.67; H, 2.56. Found: C, 45.62; H, 2.60. IR (KBr) ν_{max}: 3337 cm^{-1} (s, ν_{O-H}), 1634 cm^{-1} (s, $\nu_{C=O}$), 1327 cm^{-1} (s), 1279 cm^{-1} (s), 1125 cm^{-1} (s, ν_{C-F}), 753 cm^{-1} (m, ν_{CF_3}).

Synthesis of 2, 3, 5, and 6. Complexes **2**, **3**, **5**, and **6** were prepared by stirring equimolar solutions of $Ln(TFI)_3(H_2O)_2$ and the nitrogen donor in CH_3OH for 24 h at room temperature. The products were isolated and purified following the aforementioned method. The single crystals were harvested in about two weeks by recrystallization from chloroform/hexane.

$Eu(TFI)_3(bpy)$ (2). Yield: 91%. Elemental analysis (%) calcd for $C_{43}H_{26}EuF_9N_2O_6$ (989.62): C, 52.19; H, 2.65; N, 2.83. Found: C, 52.16; H, 2.62; N, 2.82. IR (KBr) ν_{max}: 1632 cm^{-1} (s, $\nu_{C=O}$), 1327 cm^{-1} (s), 1281 cm^{-1} (s), 1128 cm^{-1} (s, ν_{C-F}), 755 cm^{-1} (m, ν_{CF_3}).

$[Eu(TFI)_3(phen)]{\cdot}CHCl_3$ (3). Yield: 89%. Elemental analysis (%) calcd for $C_{46}H_{27}Cl_3EuF_9N_2O_6$ (1131.01): C, 48.76; H, 2.40; N, 2.47. Found: C, 48.75; H, 2.38; N, 2.44. IR (KBr) ν_{max}: 1635 cm^{-1} (s, $\nu_{C=O}$), 1327 cm^{-1} (s), 1280 cm^{-1} (s), 1126 cm^{-1} (s, ν_{C-F}), 755 cm^{-1} (m, ν_{CF_3}).

$Sm(TFI)_3(bpy)$ (5). Yield: 93%. Elemental analysis (%) calcd for $C_{43}H_{26}SmF_9N_2O_6$ (988.01): C, 52.21; H, 2.65; N, 2.84. Found: C,

dx.doi.org/10.1021/ic202473b | Inorg. Chem. 2012, 51, 5050−5057

Scheme 2. Synthesis of Complexes 1−6

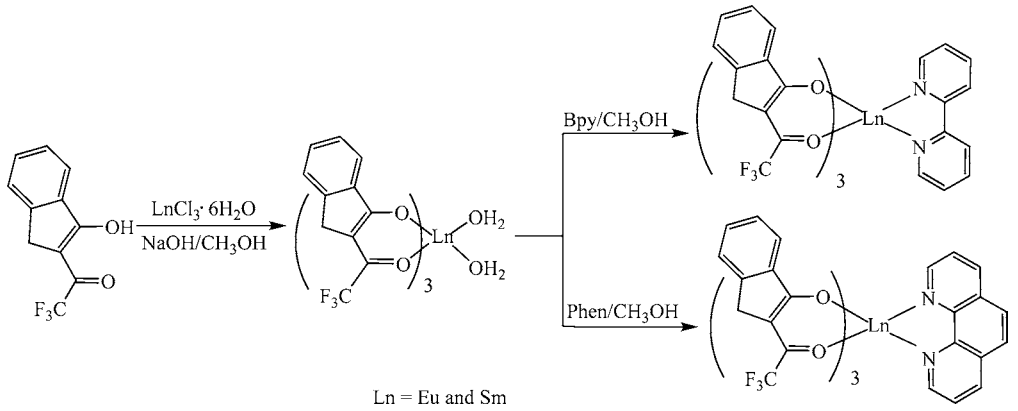

Table 1. Crystal Data and Structure Refinement for Complexes 1−6

param.	1	2	3	4	5	6
formula	$C_{33}H_{22}EuF_9O_8$	$C_{43}H_{26}EuF_9N_2O_6$	$C_{46}H_{27}EuCl_3F_9N_2O_6$	$C_{33}H_{22}SmF_9O_8$	$C_{43}H_{26}SmF_9N_2O_6$	$C_{46}H_{27}SmCl_3F_9N_2O_6$
formula weight	869.47	989.62	1132.98	867.86	988.01	1131.40
color	buff	buff	buff	buff	buff	buff
cryst syst	monoclinic	monoclinic	triclinic	monoclinic	monoclinic	triclinic
space group	$C2/c$	$P2_1$	$P\bar{1}$	$C2/c$	$P2_1$	$P\bar{1}$
a (Å)	24.112(5)	11.034(2)	10.061(2)	23.943(5)	11.018(2)	10.063(2)
b (Å)	15.070(3)	9.1616(18)	14.690(3)	15.055(3)	9.1465(18)	14.692(3)
c (Å)	18.375(4)	19.840(4)	16.362(3)	18.355(4)	19.800(4)	16.379(3)
α (deg)	90	90	100.68(3)	90	90	100.54(3)
β (deg)	92.90(3)	95.60(3)	93.26(3)	92.98(3)	95.80(3)	93.40(3)
γ (deg)	90	90	106.81(3)	90	90	106.75(3)
V (Å^3)	6668(2)	1996.0(7)	2259.1(8)	6607(2)	1985.2(7)	2263.5(8)
Z	8	2	2	8	2	2
ρ (g cm^3)	1.732	1.647	1.661	1.745	1.653	1.660
μ (mm^{-1})	1.982	1.664	1.653	1.879	1.572	1.562
F (000)	3423	980	1114	3416	978	1118
R_1, [$I > 2\sigma$ (I)]	0.0476	0.0339	0.0543	0.0333	0.0448	0.0446
wR_2, [$I > 2\sigma$ (I)]	0.1127	0.0819	0.1261	0.0844	0.1015	0.1120
$R1$, (all data)	0.0704	0.0381	0.0925	0.0454	0.0552	0.0545
wR_2, (all date)	0.1238	0.0855	0.1892	0.0891	0.1063	0.1181
GOF on F^2	1.066	1.081	1.157	1.076	1.087	1.034

52.24; H, 2.62; N, 2.85. IR (KBr) ν_{max}: 1631 cm^{-1} (s, $\nu_{C=O}$), 1328 cm^{-1} (s), 1280 cm^{-1} (s), 1127 cm^{-1} (s, ν_{C-F}), 754 cm^{-1} (m, ν_{CF_3}).

[Sm(TFI)$_3$(phen)]·CHCl$_3$ (6). Yield: 88%. Elemental analysis (%) calcd for $C_{46}H_{27}Cl_3SmF_9N_2O_6$ (1131.40): C, 48.83; H, 2.41; N, 2.48. Found: C, 48.85; H, 2.39; N, 2.49. IR (KBr) ν_{max}: 1634 cm^{-1} (s, $\nu_{C=O}$), 1329 cm^{-1} (s), 1281 cm^{-1} (s), 1127 cm^{-1} (s, ν_{C-F}), 754 cm^{-1} (m, ν_{CF_3}).

Determination of the Crystal Structures. Suitable single crystals of **1**−**6** were selected for X-ray diffraction analysis. Structural analyses were performed on a Siemens SMART CCD diffractometer using graphite-monochromated Mo Kα radiation (λ = 0.71073 Å). Data processing was accomplished with the SAINT processing program. All data were collected at a temperature of 20 ± 2 °C. The structures were solved by the direct methods and refined on F^2 by full-matrix least-squares using the SHELXTL-97 program. The Ln^{3+} ions were easily located, and then non-hydrogen atoms (C, N, O, and F) were placed from the subsequent Fourier-difference maps. All non-hydrogen atoms were refined anisotropically.

RESULTS AND DISCUSSION

Synthesis and Spectral Analysis of Complexes 1−6. Complexes **1**−**6** are synthesized following the Scheme 2. The IR spectra of both complexes **1** and **4** exhibit the typical broad absorption in the region 3000−3500 cm^{-1}, which is consistent with the presence of water molecules in the complexes **1** and **4**. On the contrary, the absence of the broad band in the region 3000−3500 cm^{-1} for complexes **2**, **3**, **5**, and **6** suggests that water molecules have been displaced by the bidentate neutral donors.[23] It is clear from the thermogravimetric analysis data that complex **1** undergoes a mass loss of about 4% (calcd 4.1%) in the first step (97−135 °C), which corresponds to the loss of the coordinated water molecules, and then, it undergoes a single step decomposition (Figure S3, Supporting Information). In contrast, complexes **2** and **3** are more stable than complex **1**, and they undergo single-step decomposition at 260 °C, hinting that there are no solvents in the complexes **2** and **3** (Figures S4 and S5, Supporting Information). Thermogravimetry differential scanning calorimetry (TG−DSC) curves of complexes **4**−**6** are similar to those of complexes **1**−**3** (Figures S6, S7, and S8, Supporting Information).

X-ray Structural Characterization. X-ray crystallographic analysis reveals that complexes **1** and **4**, complexes **2** and **5**, complexes **3** and **6** are isostructural, respectively. Crystal data and data collection parameters for complexes **1**−**6** are given in Table 1. The selected bond lengths and angles for complexes

dx.doi.org/10.1021/ic202473b | Inorg. Chem. 2012, 51, 5050−5057

1−**6** are given in Table S1 in the Supporting Information. In a typical structure of complex **1**, (Figure 1) each central Eu^{3+} ion

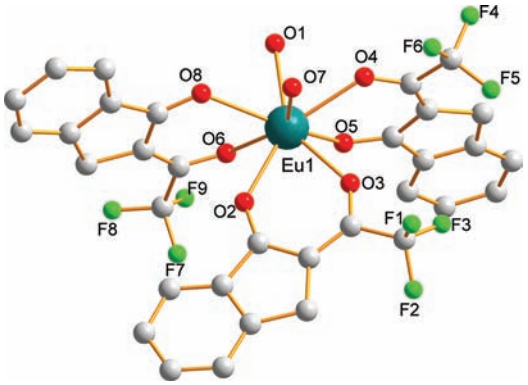

Figure 1. Molecular structure of complex **1**.

is coordinated by six oxygen atoms from three TFI ligands and two oxygen atoms from H_2O, resulting in the bicapped trigonal prism geometry. It is consistent with previously reported analogue.[24] The average bond length of the Eu−O (TFI oxygen atoms) is 2.385 Å, which is slightly shorter than that of Eu−O (water oxygen atom, 2.452 Å). It is attributed to that the ionic bond of Eu−O (TFI oxygen atoms) is stronger than the covalent bond of Eu−O (water oxygen atom).

In the structure of complexes **2** and **3**, (Figure 2) two water molecules are substituted by the ancillary ligand of bpy and phen so that each central Eu^{3+} ion is coordinated by six oxygen atoms from three TFI ligands and two nitrogen atoms from bpy and phen ligand, respectively. The coordination geometry of Eu^{3+} ion in **2** and **3** can be described as a distorted square antiprism and bicapped trigonal prism, respectively. In complex **2**, the average bond distances of Eu−N and Eu−O are 2.603 Å and 2.367 Å, respectively, which are similar to those in complex **3**, where the average bond distances of Eu−N and Eu−O are 2.594 Å and 2.370 Å, respectively. The asymmetric unit and coordination geometry of complexes **4**−**6** are given in Figures S9−S11 in the Supporting Information.

UV−Vis Spectra. The UV−vis absorption spectra of the free ligand TFI, NaTFI, and complexes **1**−**3** were measured in CH_3CN solution ($c = 1 \times 10^{-5}$ M). (Figure 3) The absorption

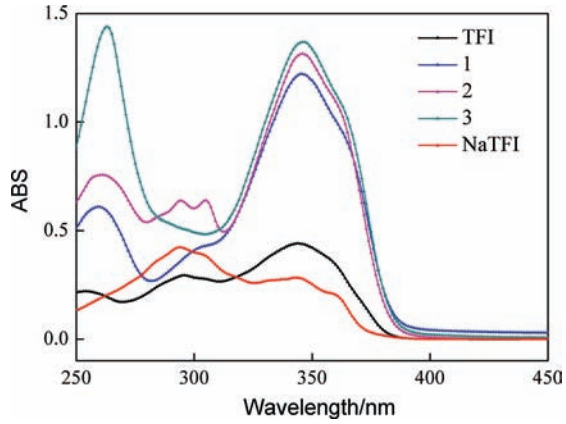

Figure 3. UV−vis absorption spectra of TFI, NaTFI and complexes **1**−**3** in CH_3CN ($c = 1 \times 10^{-5}$ M).

hump bands for NaTFI and TFI are observed at the same position (294 and 342 nm). However, their maximum absorption hump bands (294 nm for NaTFI, 342 nm for TFI) are different, which is attributed to the proton effect. The maximum absorption hump bands are observed at 342 nm for TFI and at around 345 nm for complexes **1**−**3**, which are attributed to singlet−singlet $\pi-\pi^*$ enol absorption of β-diketonate ligand. In comparison with the maximum absorption of TFI, the absorption maxima are slightly red-shifted 3 nm for complexes **1**−**3**, which is attributed to the perturbation induced by the coordination of Eu^{3+} ion. However, the spectral patterns of the complexes **1**−**3** in CH_3CN are similar to that of the free ligands, suggesting that the coordination of Eu^{3+} ions has no significant influence on the $^1\pi-\pi^*$ state energy. The determined molar absorption coefficient values of complexes **1**−**3** at 345 nm, 1.21×10^4, 1.24×10^4, and 1.27×10^4 $L \cdot mol^{-1} \cdot cm^{-1}$, respectively, are about 3 times higher than that of the TFI (4.20×10^3 $L \cdot mol^{-1} \cdot cm^{-1}$ at 342 nm), proposing the presence of three β-diketonate ligands in the corresponding complexes. Obviously, the absorption intensity is in the sequence of **3** > **2** > **1**, which corresponds with the conjugation extent in complexes **1**−**3**.

Photoluminescence (PL) Properties of Complexes 1−**6.** PL spectra of complexes **1**−**3** in CH_3CN are shown in Figure

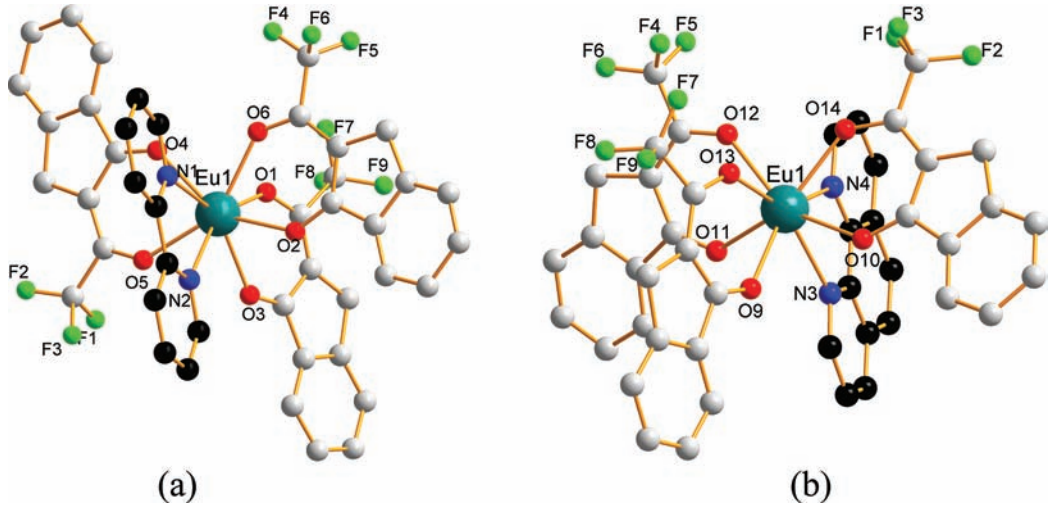

Figure 2. Molecular structure of (a) complex **2** and (b) complex **3**.

dx.doi.org/10.1021/ic202473b | *Inorg. Chem.* 2012, 51, 5050−5057

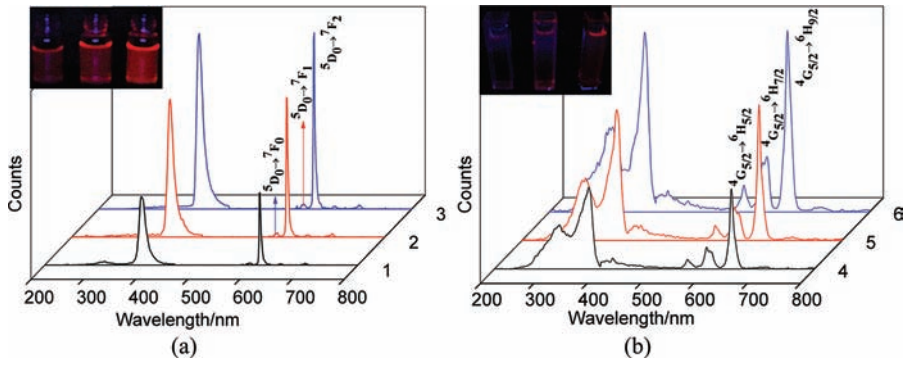

Figure 4. PL spectra of complexes (a) **1**–**3** in CH_3CN ($c = 1 \times 10^{-5}$ M) and (b) **4**–**6** in CH_3CN ($c = 1 \times 10^{-5}$ M).

Table 2. Radiative (A_{RAD}) and Nonradiative (A_{NR}) Decay Rates, Observed Luminescence Lifetime (τ_{obs}), Intrinsic Quantum Yield (Φ_{ln}), Sensitization Efficiency (Φ_{sens}), and Overall Quantum Yield ($\Phi_{overall}$) for Complexes 1–3 and the Reported Analogous Lanthanide Complexes at 298 K

complexes	A_{RAD} (s^{-1})	A_{NR} (s^{-1})	τ_{obs} (μs)	Φ_{ln} (%)	Φ_{sens} (%)	$\Phi_{overall}$ (%)
$Eu(TFI)_3(H_2O)_2$ (**1**)	2540	19740	45	12	45	6.5
$Eu(PBI)_3(C_2H_5OH)(H_2O)$[20]	1059	2941	250	26	8.0	2.2
$Eu(PFNP)_3(C_2H_5OH)(H_2O)$[9b]	899	557	687	62	10	6.0
$Eu(TFI)_3(bpy)$ (**2**)	2160	9708	84	18	74	13.5
$Eu(PBI)_3(bpy)$[20]	6911	3314	978	68	22	15
$Eu(PFNP)_3(bpy)$[9b]	560	248	1238	69	23	16
$Eu(TFI)_3(phen)$ (**3**)	1920	5884	128	25	76	18.6
$Eu(PBI)_3(phen)$[20]	5543	4213	1025	57	20	11
$Eu(PFNP)_3(phen)$[9b]	591	255	1183	70	53	37

4a. In comparison with the absorption of complexes **1**–**6**, the excitation spectra show narrow bands around 390 nm for **1**–**3** and 375 nm for **4**–**6**. Thus, the excitation and absorbance wavelength of complexes **1**–**6** overlap very well within the range, indicating that the emissions originate from the energy absorbed by the ligands. Upon excitation at 390 nm, which is the maximum of the excitation spectrum, complexes **1**–**3** showed the characteristic narrow emission bands of the Eu^{3+} ion corresponding to the $^5D_0 \rightarrow {}^7F_J$ ($J = 0$–4) transitions. Among them, the $^5D_0 \rightarrow {}^7F_2$ transition at $\lambda = 613$ nm is the strongest emission that is an induced electric dipole transition, and its corresponding intensity is very sensitive to the coordination environment. This very intense $^5D_0 \rightarrow {}^7F_2$ peak, pointing to a highly polarizable chemical environment around the Eu^{3+} ion and is responsible for the brilliant red emission of complexes **1**–**3**.[20,25] The intensity of the emission band at 593 nm is relatively weak and independent of the coordination environment because the corresponding transition $^5D_0 \rightarrow {}^7F_1$ is a magnetic transition. The intensity ratio of I_{7F2}/I_{7F1} is 9.48 for complex **1**, while it increased to 13.30 for **2** and 12.45 for **3**, suggesting that the Eu^{3+} ion is coordinated in a local site without any inversion center. Further, the emission spectra of complexes **1**–**3** show only one peak for the $^5D_0 \rightarrow {}^7F_0$ transition and three stark components for the $^5D_0 \rightarrow {}^7F_1$ transition, indicating the presence of a single chemical environment around the Eu^{3+} ion. The emission bands around 580 and 650 nm are very weak, since their corresponding transitions $^5D_0 \rightarrow {}^7F_{0,3}$ are forbidden both in magnetic and electric dipole schemes. The solid PL spectra of complexes **1**–**3** recorded at 303 K are shown in Figures S12–S14 in the Supporting Information. PL spectra of complexes **4**–**6** in CH_3CN are shown in Figure 4b. Upon excitation at 375 nm, which is the maximum of the excitation spectrum, complexes **4**–**6** show characteristic narrow band emissions of Sm^{3+} ion corresponding to the $^4G_{5/2} \rightarrow {}^6H_J$ ($J = {}^5/_2, {}^7/_2, {}^9/_2, {}^{11}/_2$) transitions. The three expected peaks for the $^4G_{5/2} \rightarrow {}^6H_{5/2-9/2}$ transitions are well resolved. The most intense peak is the hypersensitive transition $^4G_{5/2} \rightarrow {}^6H_{9/2}$ at 644 nm.

The $^5D_0$ lifetime (τ_{obs}) were determined from the luminescent decay profiles for complexes **1**–**3** at room temperature by fitting with monoexponential curves, proposing the presence of single chemical environment around the emitting Eu^{3+} ion, and the values are depicted in Table 2. Typical decay profiles of complexes **1**–**3** are shown in Figure S15 in the Supporting Information. The relatively shorter lifetime observed for complex **1** ($\tau_{obs} = 45$ μs) can be caused by dominant nonradiative decay channels associated with vibronic coupling because of the presence of water molecules, as well documented in many of the hydrated europium β-diketonate complexes. On the other hand, the relative longer lifetimes have been observed for complexes **2** ($\tau_{obs} = 84$ μs) and **3** ($\tau_{obs} = 128$ μs) because of less important nonradiative deactivation pathways. The lifetime observed for complexes **4** ($\tau_{obs} = 13$ μs), **5** ($\tau_{obs} = 29$ μs), and **6** ($\tau_{obs} = 70$ μs) are relatively shorter than those of Eu^{3+} complexes. The decay profiles of complexes **4**–**6** are shown in Figure S16 in the Supporting Information.

The overall quantum yield ($\Phi_{overall}$) for a lanthanide complex treats the system as a "black box", in which the internal process is not explicitly considered. Given that the complex absorbs a photon, the overall quantum yield can be defined as eq 2.[26]

$$\Phi_{sens} = \frac{\Phi_{overall}}{\Phi_{Ln}} \tag{2}$$

Here, $\Phi_{transfer}$ is the efficiency of energy transfer from the ligand to Eu^{3+} ions, and Φ_{Ln} represents the intrinsic quantum yield of the lanthanide ion, which can be calculated as eq 3.[27]

dx.doi.org/10.1021/ic202473b | Inorg. Chem. 2012, 51, 5050–5057

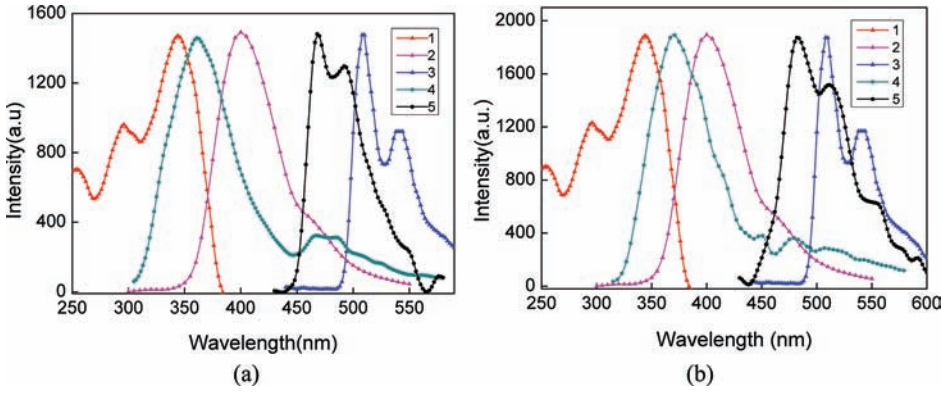

Figure 5. (a) (1) UV–vis absorption spectrum of TFI. (2) Room temperature emission spectrum of TFI. (3) Phosphorescence spectrum of $[Gd(TFI)_3(H_2O)_2]$ at 77 K. (4) Room temperature emission spectrum of bpy. (5) Phosphorescence spectrum of $Gd(bpy)_2(NO_3)_3$ at 77 K. (b) (1) UV–Vis absorption spectrum of TFI. (2) Room temperature emission spectrum of TFI. (3) Phosphorescence spectrum of $[Gd(TFI)_3(H_2O)_2]$ at 77 K. (4) Room temperature emission spectrum of phen. (5) Phosphorescence spectrum of $Gd(phen)_2(NO_3)_3$ at 77 K.

$$\Phi_{Ln} = \frac{A_{RAD}}{A_{RAD} + A_{NR}} = \frac{\tau_{obs}}{\tau_{rad}} \quad (3)$$

The radiative lifetime (τ_{rad}) can be calculated using eq 4,[28] assuming that the energy of the $^5D_0 \rightarrow {}^7F_1$ transition (MD) and its oscillator strength are constant.

$$A_{RAD} = \frac{1}{\tau_{rad}} = A_{MD,0} n^3 \left(\frac{I_{tot}}{I_{MD}}\right) \quad (4)$$

where $A_{MD,0}$ = 14.65 s^{-1} is the spontaneous emission probability of the magnetic dipole $^5D_0 \rightarrow {}^7F_1$ transition, n is the refractive index of the medium, I_{tot} is the total integrated emission of the $^5D_0 \rightarrow {}^7F_J$ transitions, and I_{MD} is the integrated emission of the $^5D_0 \rightarrow {}^7F_1$ transition. A_{RAD} and A_{NR} are radiative and nonradiative decay rates, respectively.

The corresponding parameters of the photophysical properties for solution samples of complexes **1**–**3** are summarized in Table 2. The overall luminescence quantum yield ($\Phi_{overall}$) observed for complex **1** is the lowest among the three complexes. It is understandable that the presence of the O–H oscillators in close proximity to the Eu^{3+} ion center effectively quenches the luminescence *via* vibrational relaxations.[29] On the other hand, the substitution of the solvent molecules by the bidentate nitrogen donors in complexes **2** and **3** leads to an increase in the observed quantum yields. Thus, the complexes **1**–**3** show the increasing luminescence quantum yields in a sequence of **1** < **2** < **3**, which is consistent with the literature.[30] In comparison with the luminescence quantum yields reported in the literature (Table 2), the overall quantum yield of complex **3** ranks the second among their analogues of complexes $Eu(PBI)_3L$ and $Eu(PFNP)_3L$ (PBI = 3-phenyl-4-benzoyl-5-isoxazolone, PFNP = 4,4,5,5,5-pentafluoro-1-(naphthalen-2-yl)pentane-1,3-dione, L = H_2O/C_2H_5OH, bpy, and phen). Obviously, the sensitization efficiency (Φ_{sens}) of TFI to Eu^{3+} ion in complexes **1**–**3** is found to be promising.

Intramolecular Energy Transfer between Ligands and Eu^{3+} Ion. In general, the widely accepted energy transfer mechanism in lanthanide complexes is proposed by Crosby.[31–34] In order to make energy transfer effective, the energy level match between the triple states of the ligands and the $^5D_0$ of the Eu^{3+} ion becomes one of the most important factors dominating the luminescence properties of the europium complexes. To elucidate the energy transfer processes in the europium complexes, the energy levels of the relevant electronic states should be estimated. The singlet and triplet energy levels of TFI and bidentate nitrogen donors are estimated by referring to their wavelengths of UV–vis absorbance edges and the lower wavelength emission peaks of the corresponding phosphorescence spectra. On account of the difficulty in observing the phosphorescence spectra of the ligand, the emission spectra of the complex $Gd(TFI)_3(H_2O)_2$ at 77 K can be used to estimate the triplet state energy level. Because the lowest excited energy level of the Gd^{3+} cation ($^6P_{7/2}$) is too high to accept energy transfer from the ligands, the triplet state energy level of the ligand is not significantly affected by the Gd^{3+} ion. As shown in Figure 5, the triplet energy level of $Gd(TFI)_3(H_2O)_2$, which corresponds to the lower emission peak wavelength, is 19 607 cm^{-1} (510 nm). The single state energy ($^1\pi\pi^*$) level of TFI is estimated by referencing its absorbance edge, which is 25 641 cm^{-1} (390 nm). The singlet and triplet energy levels of bpy (29 900 and 22 900 cm^{-1}) and phen (31 000 and 22 100 cm^{-1}) were taken from the literature.[35,36] The triplet (T_1) energy levels are calculated[37] by referring to the lower wavelength emission peaks of the corresponding phosphorescence spectra of Gd^{3+} complex as in Figure 5. Accordingly, the triplet energy levels of the ligand TFI is found to be 19 607 cm^{-1} (510 nm).

It is well-known that neutral ligands often play two major roles in luminescent lanthanide complexes; for example, one is to replace the coordination solvent molecules for minimizing the nonradiative deactivation, the other one is to play the antenna role, absorbing light and transferring excitation energy to the other ligands or to the emitting ion. To better understand the energy transfer process between the primary ligand TFI and the neutral ligands, the overlap of the absorption and photoluminescence spectra of TFI and bidentate nitrogen donors should be discussed in detail. In a typical example of complex **2**, there is an overlap between the room temperature emission spectrum of bpy and the absorption spectra of the TFI in the region 300–383 nm (Figure 5a). It indicates that the radiative energy that comes from the singlet state of bpy can in part be absorbed by TFI. The singlet state of bpy can also transfer energy to the triplet level of TFI or to its own triplet level, which can be proved from the overlap between the room temperature emission of bpy and the phosphorescence spectra of $Gd(TFI)_3(H_2O)_2$ and $Gd(bpy)_2(NO_3)_3$. The singlet level of the TFI can transfer energy to the triplet state of bpy or to its own triplet level

dx.doi.org/10.1021/ic202473b | *Inorg. Chem.* 2012, 51, 5050–5057

(overlap between the room temperature emission of TFI and the phosphorescence spectra of bpy or TFI). The triplet level of neutral ligand, bpy can also transfer energy to the central Eu^{3+} ion directly or through the triplet state of TFI (overlap of the phosphorescence spectra of $Gd(TFI)_3(H_2O)_2$ and $Gd(bpy)_2(NO_3)_3$). Similar processes can be observed for complex **3** (Figure 5b).

According to the above experimental results, the schematic energy level diagram and the energy transfer process that possibly takes place in complex **2** is shown in Figure 6. The

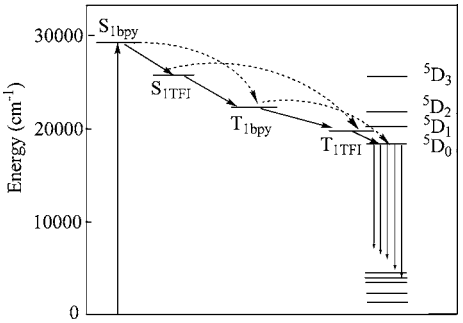

Figure 6. Schematic energy level diagram and energy transfer process for complex **2**. S1, first excited singlet state; T1, first excited triplet state.

triplet levels of the ligand TFI (19 607 cm^{-1}), bpy (22 900 cm^{-1}), and phen (22 100 cm^{-1}) are obviously higher than the $^5D_0$ level (17 500 cm^{-1}) of Eu^{3+} ion, and their energy gaps ΔE ($^3\pi\pi^*-^5D_0$) are 2107, 3867, and 3290 cm^{-1}, respectively, which are too high to allow an effective back energy transfer. The energy gap between the $^1\pi\pi^*$ and $^3\pi\pi^*$ states of TFI, bpy, and phen are 6034, 8533, and 10210 cm^{-1}, respectively. According to Reinhoudt's empirical rule, the intersystem crossing process becomes effective when ΔE ($^1\pi\pi^*-^3\pi\pi^*$) is at least 5000 cm^{-1}.[38] Therefore, the effective intersystem crossing and ligand to metal energy transfer processes can be found in all complexes **1**–**3**, which demonstrated that the ligands are suitable for sensitizing the Eu^{3+} ion luminescence.

CONCLUSIONS

We have designed and synthesized a new β-diketone, 2-(2,2,2-trifluoroethyl)-1-indone (TFI), which is a promising luminescence sensitizer on lanthanide ions, on the basis of trifluorinated alkyl group and a rigid indone group. Isolation and structural characterization of two series of Eu^{3+} and Sm^{3+} complexes as well as systematic investigations on their photophysical properties further demonstrate that the TFI ligand is an effective sensitizer on luminescence of Eu^{3+} ions. And the ancillary bidentate nitrogen ligands can effectively enhance the luminescence quantum yields and lifetimes of Eu^{3+} ions.

ASSOCIATED CONTENT

Supporting Information

Crystallographic data for complexes **1**–**6**, NMR spectrum for the HTFI, EI-MS spectrum for TFI, TG-DSC curves for complexes **1**–**6**, PL spectra of complexes **1**–**3** in solid state, luminescence decay profiles of complexes **1**–**6**, additional figures, and CCDC Nos. 841817–841822 contain supplementary crystallographic data for complexes **1**–**6**. This material is available free of charge via the Internet at http://pubs.acs.org.

AUTHOR INFORMATION

Corresponding Author

*E-mail: yanpf@vip.sina.com (P.Y.); gmli_2000@163.com (G.L.).

Notes

The authors declare no competing financial interest.

ACKNOWLEDGMENTS

This work is financially supported by the National Natural Science Foundation of China (Nos. 21072049 and 21072050), Heilongjiang Province (No. 2010td03), and Heilongjiang University (Nos. 2010hdtd-08 and 2010hdtd-11).

REFERENCES

(1) Yu, J. B.; Zhou, L.; Zhang, H. J.; Zheng, Y. X.; Li, H. R.; Deng, R. P.; Peng, Z. P.; Li, Z. F. *Inorg. Chem.* **2005**, *44*, 1611–1618.

(2) (a) Zucchi, G.; Murugesan, V.; Tondelier, D.; Aldakov, D.; Jeon, T.; Yang, F.; Thuéry, P.; Ephritikhine, M.; Geffroy, B. *Inorg. Chem.* **2011**, *50*, 4851–4856. (b) Freund, C.; Porzio, W.; Giovanella, U.; Vignali, F.; Pasini, M.; Destri, S. *Inorg. Chem.* **2011**, *50*, 5417–5429. (c) Wang, H. H.; He, P.; Yan, H. G.; Gong, M. L. *Sens. Actuators, B* **2011**, *156*, 6–11.

(3) (a) Piazza, E. D.; Norel, L.; Costuas, K.; Bourdolle, A.; Maury, O.; Rigaut, S. *J. Am. Chem. Soc.* **2011**, *133*, 6174–6176. (b) Bünzli, J.-C. G. *Chem. Rev.* **2010**, *110*, 2729–2755. (c) Shao, G. S.; Han, R. C.; Ma, Y.; Tang, M. X.; Xue, F. M.; Sha, Y. L.; Wang, Y. *Chem.—Eur. J.* **2010**, *16*, 8647–8651.

(4) (a) Shi, M.; Ding, C. R.; Dong, J. W.; Wang, H. Z.; Tian, Y. P.; Hu, Z. J. *Phys. Chem. Chem. Phys.* **2009**, *11*, 5119–5123. (b) Bünzli, J.-C. G.; Eliseeva, S. V. *Chem. Soc. Rev.* **2010**, *39*, 189–227.

(5) Jang, H.; Shin, C. H.; Jung, B. J.; Kim, D. H.; Shim, H. K.; Do, Y. *Eur. J. Inorg. Chem.* **2006**, 718–725.

(6) Wang, J. F.; Wang, R. Y.; Yang, J.; Zheng, Z. P.; Carducci, M. D.; Cayou, T. *J. Am. Chem. Soc.* **2001**, *123*, 6179–6180.

(7) (a) Biju, S.; Reddy, M. L. P.; Cowley, A. H.; Vasudevan, K. V. *Cryst. Growth Des.* **2009**, *9*, 3562–3569. (b) Quici, S.; Cavazzini, M.; Marzanni, G.; Accorsi, G.; Armaroli, N.; Ventura, B.; Barigelletti, F. *Inorg. Chem.* **2005**, *44*, 529–537. (c) De Silva, C. R.; Li, J.; Zheng, Z. P.; Corrales, L. R. *J. Phys. Chem. A* **2008**, *112*, 4527–4530. (d) dos Santos, E. R.; Freire, R. O.; da Costa, N. B., Jr.; Almeida Paz, F. A.; de Simone, C. A.; Júnior, S. A.; Araújo, A. A. S.; Nunes, L. A. O.; de Mesquita, M. E.; Rodrigues, M. O. *J. Phys. Chem. A* **2010**, *114*, 7928–7936.

(8) Svetlana, V. E.; Jean-Claude, G. B. *New J. Chem.* **2011**, *35*, 1165–1176.

(9) (a) Shen, L.; Shi, M.; Li, F. Y.; Zhang, D. Q.; Li, X. H.; Shi, E. X.; Yi, T.; Do, Y. K.; Huang, C. H. *Inorg. Chem.* **2006**, *45*, 6188–6197. (b) Ambili Raj, D. B.; Bijiu, S.; Reddy, M. L. P. *Inorg. Chem.* **2008**, *47*, 8091–8100.

(10) Zheng, Y. X.; Lin, J.; Lin, Q.; Yu, Y. N.; Meng, Q. G.; Zhou, Y. H.; Wang, S. B.; Wang, H. Y.; Zhang, J. *J. Mater. Chem.* **2001**, *11*, 2615–2619.

(11) He, P.; Wang, H. H.; Liu, S. G.; Shi, J. X.; Wang, G.; Gong, M. L. *Inorg. Chem.* **2009**, *48*, 11382–11387.

(12) Jenekhe, S. A.; Osaheni, J. A. *Chem. Mater.* **1994**, *6*, 1906–1909.

(13) Bassett, A. P.; Magennis, S. W.; Glover, P. B.; Lewis, D. J.; Spencer, N.; Parsons, S.; Williams, R. M.; Cola, L. D.; Pikramenou, Z. *J. Am. Chem. Soc.* **2004**, *126*, 9413–9424.

(14) Yan, B. *Mater. Lett.* **2003**, *57*, 2535–2539.

(15) Teotonio, E. E. S.; Brito, H. F.; Cremona, M.; Quirino, W. G.; Legnani, C.; Felinto, M. C. F. C. *Opt. Mater.* **2009**, *32*, 345–349.

(16) Pettinari, C.; Marchetti, F.; Pettinari, R.; Drozdov, A.; Troyanov, S.; Voloshin, A. I.; Shavaleev, N. M. *Dalton Trans.* **2002**, 1409–1415.

(17) Baker, M. H.; Dorweiler, J. D.; Ley, A. N.; Pike, R. D.; Berry, S. M. *Polyhedron* **2009**, *28*, 188–194.

(18) Manseki, K.; Yanagida, S. *Chem. Commun.* **2007**, 1242–1244.

(19) Fernandes, J. A.; Sá Ferreira, R. A.; Pillinger, M.; Carlos, L. D.; Gonçalves, I. S.; Ribeiro-Claro, P. J. A. *Eur. J. Inorg. Chem.* **2004**, 3913−3919.
(20) Biju, S.; Ambili Raj, D. B.; Reddy, M. L. P.; Kariuki, B. M. *Inorg. Chem.* **2006**, *45*, 10651−10660.
(21) Zheng, Y. X.; Fu, L. S.; Zhou, Y. H.; Yu, Y. N.; Wang, S. B.; Zhang, H. J. *J. Mater. Chem.* **2002**, *12*, 919−923.
(22) (a) Shi, M.; Li, F. Y.; Yi, T.; Zhang, D. Q.; Hu, H. M.; Huang, C. H. *Inorg. Chem.* **2005**, *44*, 8929−8936. (b) Xu, H.; Wang, L. H.; Zhu, X. H.; Yin, K.; Zhong, G. Y.; Hou, X. Y.; Huang, W. *J. Phys. Chem. B* **2006**, *110*, 3023−3029.
(23) (a) De Silva, C. R.; Maeyer, J. R.; Wang, R. Y.; Nichol, G. S.; Zheng, Z. P. *Inorg. Chim. Acta* **2007**, *360*, 3543−3552. (b) Bellusci, A.; Barberio, G.; Crispini, A.; Ghedini, M.; Deda, M. L.; Pucci, D. *Inorg. Chem.* **2005**, *44*, 1818−1825.
(24) (a) Xu, H.; Yin, K.; Huang, W. *Chem.—Eur. J.* **2007**, *13*, 10281−10293. (b) Zheng, Y. X.; Cardinali, F.; Armaroli, N.; Accorsi, G. *Eur. J. Inorg. Chem.* **2008**, 2075−2080. (c) Petit, S.; Robert, F. B.; Pilet, G.; Reber, C.; Luneau, D. *Dalton Trans.* **2009**, 6809−6815.
(25) Werts, M. H. V.; Jukes, R. T. F.; Verhoeven, J. W. *Phys. Chem. Chem. Phys.* **2002**, *4*, 1542−1548.
(26) Xiao, M.; Selvin, P. *J. Am. Chem. Soc.* **2001**, *123*, 7067−7073.
(27) (a) Chauvin, A.-S.; Gumy, F.; Imbert, D.; Bünzli, J.-C. G. *Spectrosc. Lett.* **2004**, *37*, 517−532. (b) Chauvin, A.-S.; Gumy, F.; Imbert, D.; Bünzli, J.-C. G. *Spectrosc. Lett.* **2007**, *40*, 193−193.
(28) Viswanathan, S.; Bettenacourt-Dias, A. D. *Inorg. Chem.* **2006**, *45*, 10138−10146.
(29) (a) Peng, C. Y.; Zhang, H. J.; Yu, J. B.; Meng, Q. G.; Fu, L. S.; Li, H. R.; Sun, L. N.; Guo, X. M. *J. Phys. Chem. B* **2005**, *109*, 15278−15287. (b) Wada, Y.; Okubo, T.; Ryo, M.; Nakazawa, T.; Hasegawa, Y.; Yanagida, S. *J. Am. Chem. Soc.* **2000**, *122*, 8583−8584.
(30) (a) Fu, L.; Sá Ferreira, R. A.; Silva, N. J. O.; Fernandes, J. A.; Ribeiro-Claro, P.; Gonçalves, I. S.; de Zea Bermudez, V.; Carlos, L. D. *J. Mater. Chem.* **2005**, *15*, 3117−3125. (b) Crosby, G. A.; Alire, R. M.; Whan, R. E. *J. Chem. Phys.* **1961**, *34*, 743−748.
(31) Tanaka, M.; Yamagughi, G.; Shiokawa, J.; Yamanaka, C. B. *Chem. Soc. Jpn.* **1970**, *43*, 549−550.
(32) (a) Sato, S.; Wada, M. B. *Chem. Soc. Jpn.* **1970**, *43*, 1955−1962. (b) Haynes, A. V.; Drickamer, H. G. *J. Chem. Phys.* **1982**, *76*, 114−125.
(33) Dieke, G. H. *Spectra and Energy Levels of Rare Earth Ions in Crystals*; Wiley-Interscience: New York, 1968.
(34) Stein, G.; Wurzberg, E. *J. Chem. Phys.* **1975**, *62*, 208−213.
(35) Ambili Raj, D. B.; Francis, B.; Reddy, M. L. P.; Butorac, R. R.; Lynch, V. M.; Cowley, H. *Inorg. Chem.* **2010**, *49*, 9055−9063.
(36) Yu, X.; Su, Q. *J. Photochem. Photobiolog., A* **2003**, *155*, 73−78.
(37) Lima, P. P.; Nobre, S. S.; Freire, R. O.; Júnior, S. A.; Ferreira, R. A. S.; Pischel, U.; Malta, O. L.; Carlos, L. D. *J. Phys. Chem. C* **2007**, *111*, 17627−17634.
(38) (a) Latva, M.; Takalo, H.; Mukkala, V.-M.; Matachescu, C.; Rodriguez-Ubis, J. C.; Kankare, J. *J. Lumin.* **1997**, *75*, 149−169. (b) Steemers, F. J.; Verboom, W.; Reinhoudt, D. N.; Van der Tol, E. B.; Verhoeven, J. W. *J. Am. Chem. Soc.* **1995**, *117*, 9408−9414.